Optical Anisotropy of Uniaxially Drawn Noble-Metal-Dispersed Fluorinated Polyimide Films and Its Application to Thin Film Polarizer

Sho-ichi MATSUDA, Satoshi KOIZUMI, and Shinji ANDO*

Department of Organic & Polymeric Materials, Tokyo Institute of Technology,
Ookayama 2-12-1, Meguro-ku, Tokyo 152-8552, JAPAN
Tel : *+81-3-5734-2137, Fax* : *+81-3-5734-2889, E-mail : sando@polymer.titech.ac.jp*

Abstract : Anisotropy in optical transmittance in the visible and near-infrared region was investigated for uniaxially drawn noble-metal (Ag, Au, Pd)-dispersed fluorinated polyimide (PI) films. The films were prepared in one step operation, that is thermal curing and simultaneous uniaxial drawing of poly (amic acid) films dissolving 5.7~20 mol% of metallic dopants. The PI chains having a rod-like structure were oriented along the drawing direction during curing accompanying with the precipitation of metal-nanoparticles. Nanoparticles having elongated shapes were precipitated under controlled conditions, and they exhibit appreciable anisotropy in optical transmittance. Dichroic ratios of larger than 500 were observed for an Ag-nanoparticle dispersed PI film at wavelengths of 650-900 nm. This film can be applied to thin film polarizer for optical waveguide circuits. Although such high optical anisotropy was not obtained for Au- and Pd-dispersed PIs, crystallites having well-defined lozenge or rectangular shapes were observed for Au-dispersed PI films.
Keywords : Polyimides / Metal nanoparticle / Optical anisotropy / Uniaxial orientaion

1. Introduction

Polyimide (PI) films containing metal/metal oxide particles generated *in-situ* have been extensively studied by Taylor et al. in an attempt to synthesize materials with unique electrical, magnetic, thermal, or adhesive properties [1-4]. We have prepared five kinds of metal (Al, Cu, Pd, Ag and Au)-containing fluorinated PI films and investigated the optical properties in the visible and near-infrared regions [5]. Stookey et al. first observed large anisotropy in optical transmittance (we refer to *optical anisotropy*) in a stretched inorganic glass containing silver particles [6]. The anisotropy originates from the differences in the wavelength dispersion of the resonant absorption and/or scattering parallel and perpendicular to the longer axis of elongated Ag nanoparticles, and each peak can be shifted by changing the size and anisotropy in shape of particles [7]. Although such inorganic materials exhibit high dichroic ratios and good thermal stability, they are not easy to make into thin plates or small components due to their brittleness. On the other hand, stretched polymers containing iodine nanoparticles or dichroic dyes also exhibit desirable polarizing properties in the visible region. However, they have no polarizing properties at wavelengths above 700 nm and no thermal stability above 100°C. We have reported that uniaxially drawn poly (amic acid) film can give a highly oriented PI film with a large in-plane birefringence. A thin and flexible optical half-waveplate at 1.55 μm, which is only 14.5 μm thick, has been prepared [8]. In addition, we have developed a one-step operation method that generates Ag-nanoparticles having elongated shapes in a fluorinated PI [9,10]. The preparation method is schematically shown in Fig.1.

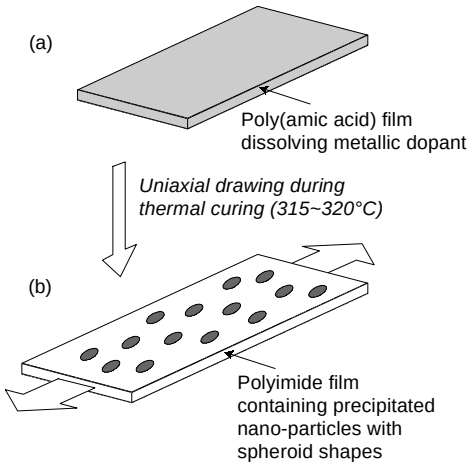

Figure 1 Method for preparing noble metal-nanoparticle-dispersed PI films.

When PI molecular chains are highly oriented by uniaxial drawing during curing, Ag-particles having elongated shapes are formed along the drawing direction so that the resulting films exhibit optical anisotropy. Scanning electron micrographs have shown that the longer axes of the elongated shapes are directed in the drawing direction [9]. In this study, the drawing procedure and curing conditions are optimized to prepare Ag-nanoparticle-dispersed PI films having large dichroic ratios and low optical losses, and we made an attempt to introduce Au- and Pd-nanoparticles into polyimide films as well.

2. Experimental

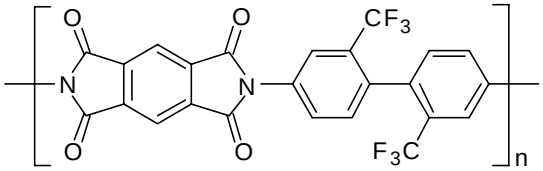

PMDA/TFDB polyimide

*2.1 Sample*s : A rigid-rod PI synthesized from pyromellitic dianhydride (PMDA) and 2,2'-bis-(trifluoromethyl)-4,4'-diaminobiphenyl (TFDB) was used in this study. This molecular structure is advantageous for generating large molecular orientation by uniaxial drawing [11,12]. In addition, this PI exhibits high transparency in the visible-near-IR region, and has high thermal stability and low water absorption (0.7 wt%) [13]. Poly (amic acid) (PAA) solution (in DMAc, 10 wt%, 600 Poise), which is the precursor of PI, was obtained from NTT-Advanced Technology Co.Ltd. Silver nitrate ($AgNO_3$), hydrogen tetrachloroaurate(III)trihydrate ($HAuCl_4 3H_2O$), and palladium(II) acetylacetonate were used as metallic dopants. These dopants have good solubility in PAA solution. DMAc solutions of PAA dissolving 5.7 (or 20) mol% of the dopants were stirred for 12 h at room temperature and spin-coated onto 3-inch silicon wafers, followed by drying in nitrogen at 70°C for 1 h. PAA films peeled from substrates were cut into rectangles of 5 x 15 mm and were uniaxially drawn during thermal curing with constant tensile loads (L) using a thermal mechanical analyzer (TMA, Sinku-Riko TM-7000). The PAA films were heated to the final curing temperature (T_f) at 10°C/min, kept at T_f for a holding time (t_H), and then cooled to room temperature. The values of T_f and t_H were set to 312–326°C and 10-180 min, respectively. The thicknesses of the resultant PI films were 13-17 μm. The PI films were uniaxially drawn up to 1.8 times of drawing ratio (R) with loads of 0.3-20 g.

2.2 Measurements : The anisotropies in optical transmittance of the metal-doped PI films were measured by rotating a Glan-Thompson prism (polarizer) inserted into the light path of a spectrophotometer (Hitachi U-3500, λ = 200-1500 nm). In-plane birefringences (Δn) of elongated PIs were measured by the parallel-Nicole rotation method at the wavelength of 1307 nm [11,12]. Thermogravimetric analysis (TGA) was conducted on small amounts (ca.10 mg) of PAA films peeled from substrates using a Shimadzu TGA-50 analyzer. PAA films were heated to 900°C at 10°C/min under N_2. Cross-sectional transmission electron (TEM) micrographs of Ag- and Au-doped PIs were taken with JEOL TEM 100CX. The uniaxially drawn PI films were embedded in epoxy resin and sectioned into a thickness of 60 nm with a Reichert-Jung Werke ultramicrotome. Wide-angle X-ray diffraction (WAXD) patterns were obtained with a two-axis X-ray diffractometer (Phillips X'Pert MPD) for PI films set on silica substrates. The diffractometer uses Cu-Kα radiation monochromatized by Si crystal. The X-ray beam scattered from the samples was detected by a scintillation counter through two receiving slits.

3. Results and Discussion

3.1 TGA Analysis of Metal-doped PAA film

Figure 2 shows the TGA profiles of undoped and Pd, Ag, and Au-doped PAA films under N_2. The weight loss below 250°C was caused by imidization reaction (evaporation of H_2O). Although the undoped PI film shows good thermal stability above 400°C, the metal-doped films show inferior

stability to the host PI. In particular, the presence of Pd and Ag compounds serves to catalyze the oxidative degradation of PI films [14]. Pd-doped PIs were excluded from the further study due to the substantial decomposition. Figure 3 shows the TGA profiles of undoped and Ag-doped PAA films. The temperature was kept constant (320°C) under N_2 and dry air after imidization reaction. The polymer decomposition was more significant in air.

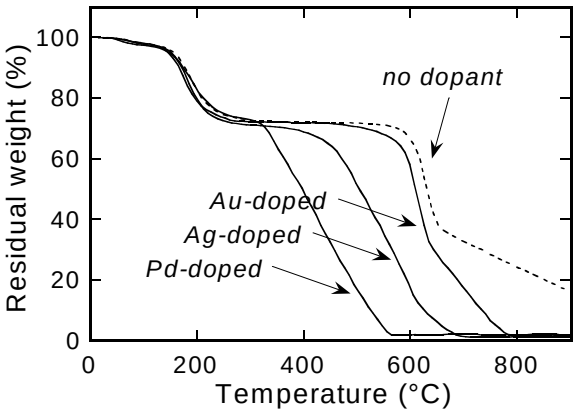

Figure 2 TGA curves of undoped and Au-, Ag-, and Pd-doped poly (amic acid) films under N_2.

3.2 Curing Atmosphere Dependence of Elongation Behaviors and Optical Properties of Ag-doped PI

We first examined the optimization of the drawing and curing conditions to prepare Ag-doped PI films having large anisotropy in optical transmittance. Figure 4 shows the temperature condition during curing and the elongation behaviors of undoped and Ag-doped PAA films under vacuum, N_2 and, air. The T_f and L were set to 320°C and 10 g, respectively. The undoped film began to shrink around 120°C and then to elongate at 200°C. This shrinkage is mainly caused by imidization [12,15]. Although Ag-doped PAA films began to shrink around 120°C, the film lengths stayed constant up to 300°C. The absence of elongation between 200°C and 300°C is related to the precipitation of Ag-nanoparticles because silver begin to precipitate at 200°C [9]. Further, the elongation behaviors above 300°C considerably depend on the atmosphere. Under vacuum, the film was gradually drawn up to a draw ratio (R) of 1.03 during the holding time at T_f. Similarly, the film was gradually drawn up to R=1.15 under N_2. The film elongation seems to be related to the polymer decomposition accompanied by Ag precipitation (Fig.3). Note that the film drawn in air was abruptly elongated in the early stage of holding time (t_H<10 min), and its length became constant at around t_H=20 min. Figure 5 shows the polarized transmission spectra of the films cured under different atmospheres. The undoped film uniaxially drawn in air shows high transmittance in a wide range (450-1300 nm) but has no optical anisotropy. All the uniaxially drawn Ag-doped films exhibited characteristic absorption around 430 nm. This wavelength coincides well with the surface plasmon resonance of Ag colloidal particles [16,17]. The films cured under vacuum and N_2 exhibit very small optical anisotropy. In contrast, the film cured in air exhibits significant anisotropy as shown in Fig.5(c). The transmittance parallel to the drawing direction ($T_{//}$) is considerably

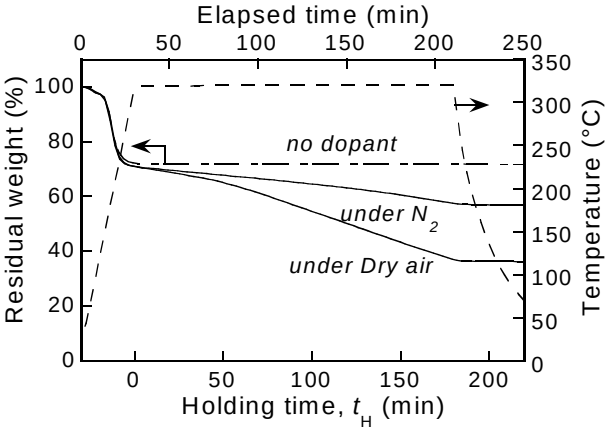

Figure 3 TGA profiles of undoped and Ag-doped PI films at 320°C under nitrogen and dry air.

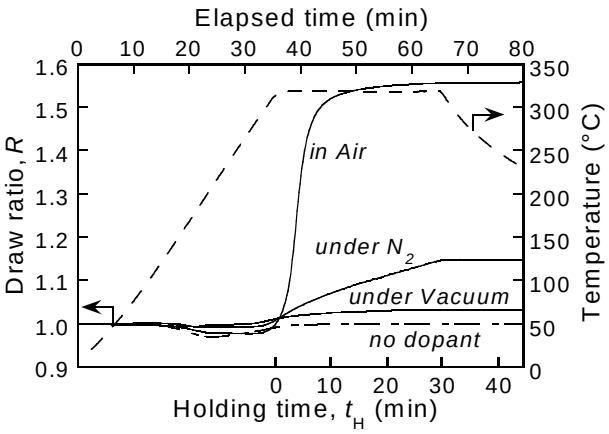

Figure 4 Elongation behavior of undoped and Ag-doped PAA films heated under vacuum, N_2 and air.

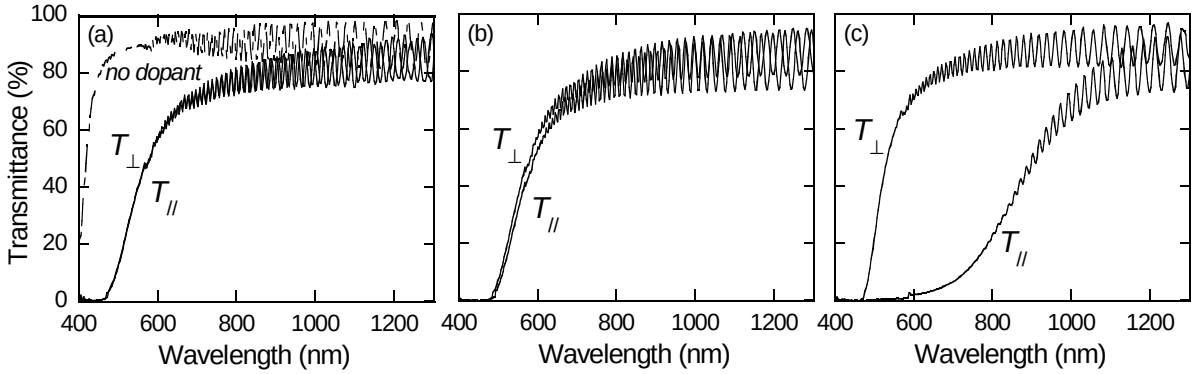

Figure 5 Polarized transmission spectra of Ag-doped PI films uniaxially drawn with a constant load (10 g) at T_f=320°C for 30 min (a) under vacuum, (b) under nitrogen and (c) in air. The spectrum of undoped PI is shown in (a) as a reference.

lower than that perpendicular to the direction ($T_\perp$). Figure 6(a) shows the dependence of in-plane birefringence (Δn) (@1307 nm) and dichroic ratio (D) (@ 670 nm) on the curing atmosphere. The molecular orientation and optical anisotropy of PIs can be quantitatively estimated by Δn and D, respectively. Small values of Δn and D were obtained under vacuum. Although a large Δn was obtained under N_2, the value of D is much smaller than that in air, suggesting that oxygen or water vapor plays an important role in the formation of Ag nanoparticles. Figure 6(b) shows the Δn and D for the films cured under mixtures of "N_2+O_2" (volume ratio 1:4), "N_2+vapor", and "N_2+O_2+vapor". Large values of Δn and D were obtained only under "N_2+O_2+vapor". Although a large Δn was obtained under "N_2+vapor", the D is much smaller. This fact indicates that water vapor promotes polymer orientation but does not affect the optical anisotropy. Consequently, O_2 seems to play an important role in the generation of large D .

Figure 7 shows the WAXD patterns of Ag-doped (20 mol%) PI films uniaxially drawn during curing under N_2 and in air. The diffraction peaks observed in both patterns at 16.2° and 17.7° are assigned to the lateral order of uniaxially oriented PI chains, and the broad signal at 24.2° is assigned to the amorphous halo of PI [18]. In addition, distinct peaks are observed for the film cured in

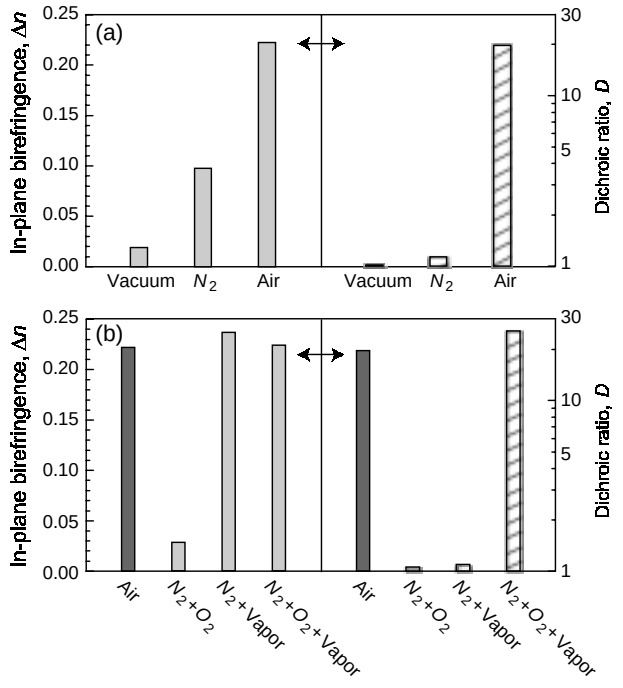

Figure 6 The dependence of the in-plane birefringence (Δn) and dichroic ratios (D) on curing atmosphere. (a) Under vacuum, nitrogen, and in air, (b) under "N_2+O_2", "N_2+vapor", and "N_2+O_2+vapor".

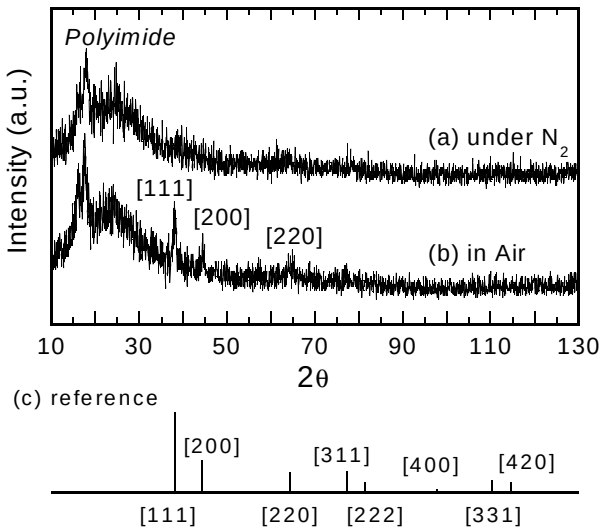

Figure 7 X-ray diffraction patterns of Ag-doped PI films prepared (a) under N_2 and (b) in air, and (c) a reference of Ag crystallites.

air, and all these peaks are assigned to those of crystalline silver (see the reference data). This indicates that $AgNO_3$ was reduced to zero-valent state (metallic silver) and crystallized in the oriented PI films.

Figure 8 shows the cross sectional TEM micrographs of Ag-doped (20 mol%) films uniaxially drawn under N_2 and in air. The precipitated Ag nanoparticles were uniformly dispersed in both of the films, but significant differences are observed in the sizes and distributions of the particles. A lot of very small (less than several nm) and relatively large (5-10 nm) spherical particles are precipitated under N_2. In contrast, much larger (10-25 nm) particles are precipitated in air, and no very small particles are observed in it. This suggests that O_2 prevents fast nucleation of Ag-crystallites. In addition, the precipitated particles in air have spheroidal shapes (aspect ratio is ca.1.5), and most of their longer axes are oriented along the drawing direction. This should be the main cause of the optical anisotropy.

3.3 Holding Time Dependence of Optical Properties.

Figure 9 shows the polarized transmission spectra of the PI films uniaxially drawn in air with varying the holding time (t_H) at a constant T_f (320°C). The wavelength dispersion of optical anisotropy shows significant dependence on t_H. Very small anisotropy is observed at t_H=19 min, and it rapidly increases until t_H=34 min. This indicates that Ag-nanoparticles grow preferentially along the drawing direction. After that (t_H>34 min), the transmittance along the drawing direction ($T_{//}$) around 600 nm gradually increases, and the anisotropy decreases. In general, the peak wavelength of the plasmon resonance is shifted in connection with the particle sizes [19]. The mechanism of the increase in $T_{//}$ at the longer t_H remains unclear, but we consider that the resonant absorption or scattering conditions were lost. In contrast to the drastic change in optical anisotropy, the values of Δn are almost constant

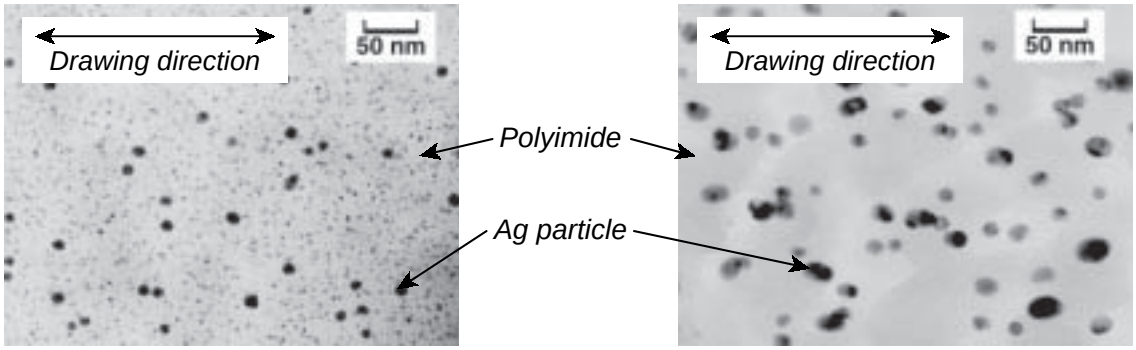

Figure 8 Cross sectional TEM micrographs (x 200,000) of Ag-doped polyimide films prepared under (a) nitrogen and (b) in air. The sectioning direction was parallel to the drawing direction.

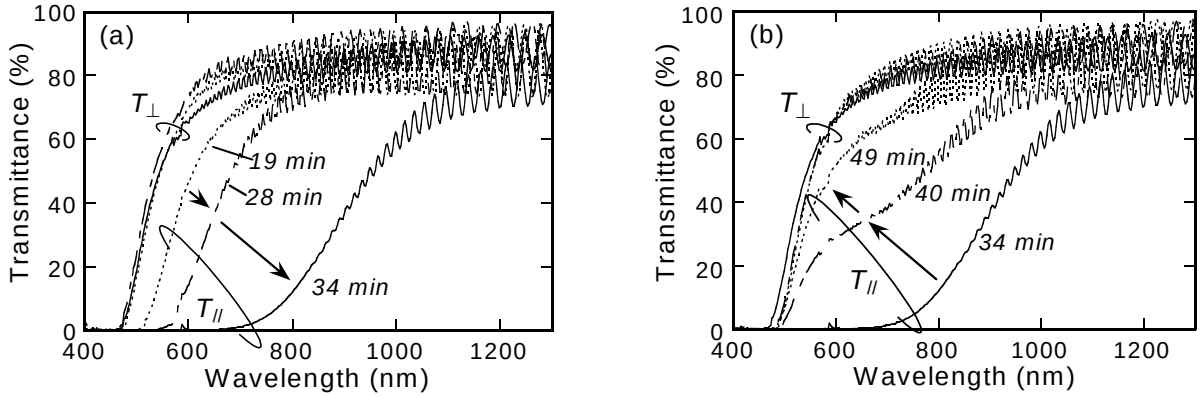

Figure 9 Polarized transmission spectra of Ag-doped PI films with varying the holding time (t_H) at T_f (320°C). (a) t_H < 34 min and (b) t_H > 34 min.

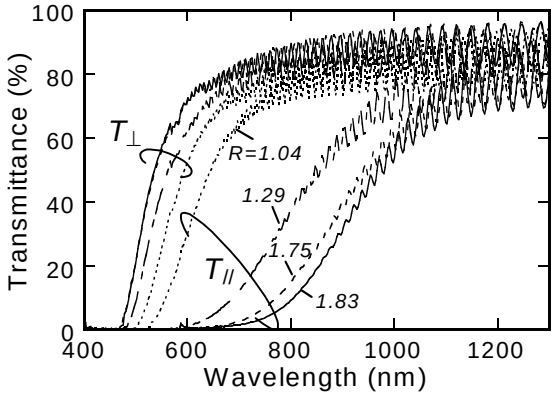

Figure 10 Polarized transmission spectra of Ag-doped PI films with varying the draw ratio (*R*).

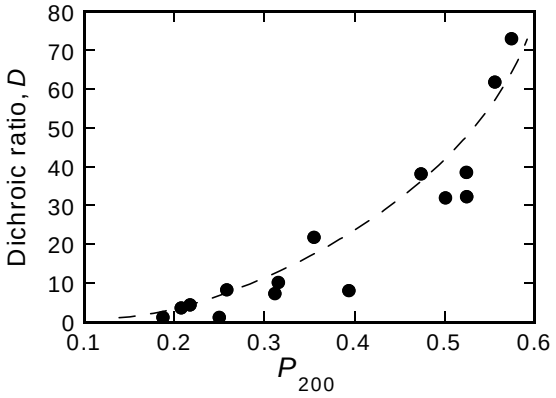

Figure 11 Orientation coefficiets (P_{200}) obtained by polarized ATR IR vs. dichroic ratios (*D*).

between t_H=19 min and t_H=60 min, indicating that the polymer orientations did not vary during curing. Hence, the decrease in anisotropy after t_H=34 min was not induced by the relaxation of polymer orientation.

3.4 Draw Ratio Dependence of Optical Properties

Figure 10 shows the polarized transmission spectra of Ag-doped PI films uniaxially drawn with varying the draw ratios (*R*) from 1.04 to 1.83. The holding time (t_H) at T_f was fixed. The transmittance in both directions ($T_{//}$ and $T_\perp$) significantly changes, and its anisotropy increases as *R* increases. This suggests that nanoparticles having larger anisotropic shapes were precipitated under the drawing conditions giving large *R* values. As shown in Figure 11, *D* is in good correlation with the polymer orientation coefficients (P_{200}) obtained by polarized ATR FT-IR method [15]. This indicates that highly oriented PI chains provide an environment that promotes the growth of Ag nanoparticles having anisotropic shapes. In other words, the optical anisotropy can be controlled by the degree of PI chain orientations.

3.5 Application to Thin Film Polarizer

Figure 12 shows the polarized transmission spectra of an Ag-doped (20 mol%) film prepared under the optimized condition. The *D* of larger than 500 and $T_\perp$ of ca.70-80 % (including surface reflection) were obtained at wavelengths between 650 and 900 nm. In addition, the film is only 14.8 μm-thick, which is sufficiently thin to reduce the excess loss caused by inserting a film into a groove formed in optical waveguides [8,20]. Inorganic plates with such thicknesses are very fragile, whereas Ag-

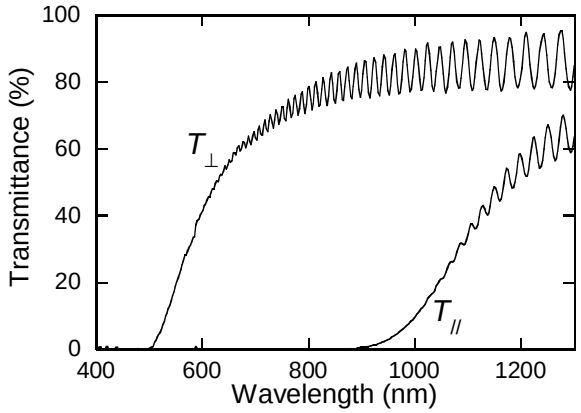

Figure 12 Polarized transmission spectra of a 14.8 μm-thick uniaxially drawn Ag-doped PI film having the largest dichroic ratio in this study.

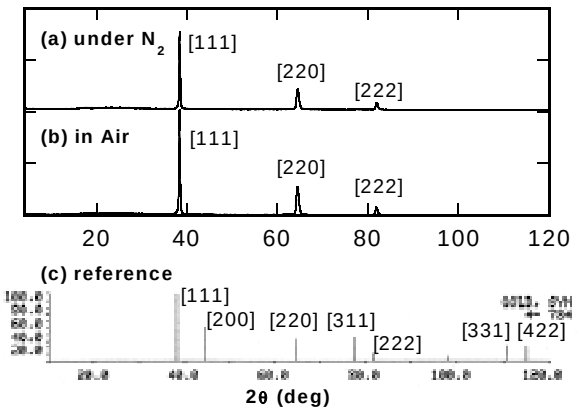

Figure 13 X-ray diffraction patterns of Au-doped PI films prepared (a) under N_2 and (b) in air, and (c) a refrenece of Au crystallites.

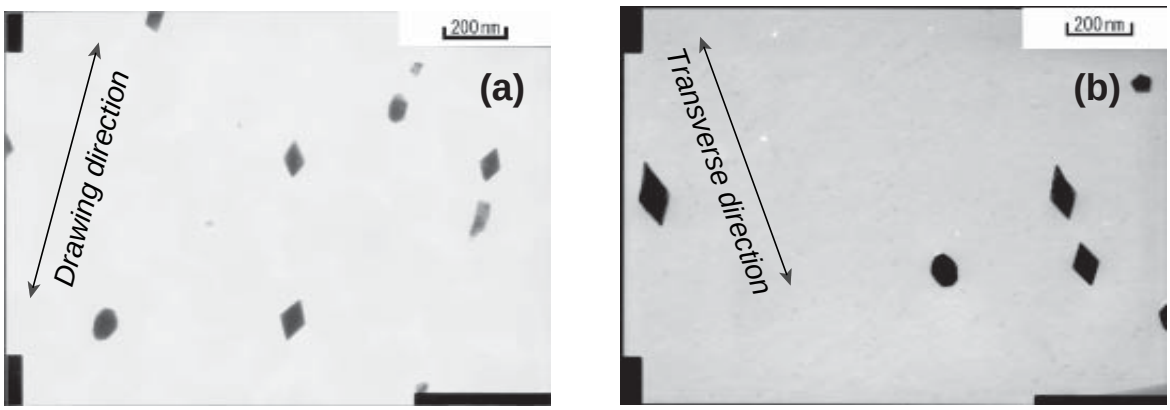

Figure 14 Cross sectional TEM micrograph (x 50,000) of Au-doped PI film prepared under N_2. The sectioning directions were (a) parallel and (b) perpendicular to the drawing direction.

doped PI films are flexible and easy to handle. Hence, a uniaxially drawn Ag-nanoparticle-dispersed PI film prepared in this study is suitable as a thin flexible polarizer for optical waveguide circuits, such as phase modulators and optical isolators.

3.6 X-ray Diffraction Patterns, TEM Micrographs and Optical Properties of Au-doped PI Films

Figure 13 shows the WAXD patterns of Au-doped PI films uniaxially drawn under N_2 and air. The T_f and t_H were set to 345°C and 120 min, respectively. All of the diffraction peaks are assigned to crystalline gold, indicating that the dopant ($HAuCl_4 3H_2O$) was reduced to zero-valent state (metallic Au) and crystallized in the PI films. Note that no peaks are observed for [200], [311], [331], and [422], which are usually observed for polycrystalline gold (see reference data). This indicates that the [111], [220], and [222] lattices of Au are preferentially formed along the film surface during curing [21].

Figures 14 shows the cross sectional TEM micrographs of an Au-doped PI film uniaxially drawn during curing under N_2. The film was sectioned along parallel ((a), *MD*) and perpendicular ((b), *TD*) to the drawing direction. A striking feature is their anisotropic and well-defined lozenge (diamond) shapes. A typical size of lozenge particles is 130 x 100 nm. In addition, most of them are oriented along the direction parallel to the surface (film plane). They are also oriented along the drawing direction (*MD*) or perpendicular to the drawing direction (*TD*). This may be related to the preferential ordering of the [111] lattice along the film surface. The similarity of the particle shapes in (a) and (b) indicates that most of the particles have pressed octahedron structures. Au-nanoparticles having rectangular shapes were observed in an Au-dispersed PI film formed on SiO_2 substrates [5], but no lozenge-shaped particles have never been observed. The micrographs of an Au-doped PI film cured in air are basically the same, while the average size of precipitated Au-particles is slightly larger.

Figure 15 shows the polarized transmission spectra of Au-doped polyimide films uniaxially drawn with constant loads. In contrast to the very pale yellow color of undoped PI, the dark purple color of

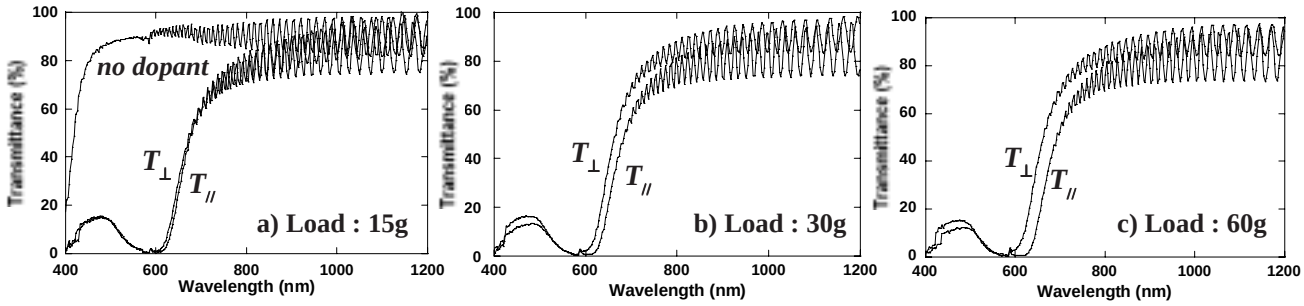

Figure 15 Polarized transmission spectra of Au-doped PI films uniaxially drawn with constant loads under N_2 at T_f =345°C for 120 min.

Au-dispersed PI films originates from the surface plasmon resonance of Au nanoparticles. This is well characterized by the strong absorptions around 600 nm. In addition, small but distinct anisotropy in optical transmission is observed for the films uniaxially drawn with large loads. This suggests that the Au-nanoparticles having anisotropic shapes are preferentially oriented along the drawing direction. In addition, the optical anisotropy should be related to the degree of orientation of polyimide chains. The investigations for the relationships among the elongation behaviors, optical properties, influence of curing atmosphere, and drawing conditions for Au-doped PI films are under way.

4. Conclusions

Anisotropy in optical transmittance was observed for uniaxially drawn and Ag- and Au-nanoparticle-dispersed PI films. The films were prepared in one step operation, that is thermal curing and simultaneous uniaxial drawing of poly (amic acid) films dissolving 5.7 (or 20) mol% of metallic dopants. The Ag- and Au-doped PI films show lower transmission in the visible region than that of host-polyimide, which is due to the resonant absorption and/or scattering of Ag- and Au-nanoparticles. Although the PI chains having a rigid-rod structure were oriented along the drawing direction during curing, large anisotropy in optical transmittance was observed only for Ag-doped PI films cured in air. The precipitated Ag-nanoparticles having spheroidal shapes were observed by TEM, and these particles were identified as zero-valent silver by X-ray diffraction. In addition, the generated optical anisotropy is very sensitive to the holding time at the final curing temperature. When Ag-doped PAA films are cured in air with the optimal holding time, the optical anisotropy is closely related to the degree of PI chain orientation. Under the optimized conditions, dichroic ratios of larger than 500 was obtained for a 14.8 μm-thick Ag-doped film at wavelengths between 650-900 nm with transmittance of 70-80 % perpendicular to the drawing direction. This film can be used as a thin-film polarizer inserted into a groove formed in optical waveguides. In a similar way, gold salt dissolved in PAA was converted into zero-valent Au-nanoparticles having high crystallinity after curing. TEM micrograph showed that the precipitated Au-nanoparticles have well-defined lozenge shapes, which suggests pressed octahedron structures of the crystallites. In addition, their longer axes are oriented along the drawing direction and the transverse direction. Although the optical anisotropy of the Au-doped films was much smaller than that of Ag-doped films, this supports the preferential orientation of Au-nanoparticles having anisotropic shapes along the drawing direction.

References

[1] Ellison MW, Taylor LT, *Chem. Mater.* 1994; **6**: 990 and the references cited therein.
[2] St. Clair AK, Taylor LT, *J. Appl. Polym. Sci*. 1983; **28**: 2393.
[3] Rancourt JD, Porta GM, Taylor LT, *Proc. 19th Intern. SAMPE Tech. Conf.* 1987; **13**: 564.
[4] Rubira AF, Rancourt JD, Caplan ML, St. Clair AK, Taylor LT, *Chem. Mater.* 1994; **6**: 2351.
[5] Sawada T, Ando S, *Chem. Mater.* 1998; **10**: 3368.
[6] Stookey SD, Araujo RJ, *Appl. Opt.* 1968; **7**: 777.
[7] Bohren CF, Huffman DR, '*Absortion and Scattering of Light by Small Particles*', John Wiley&Sons (1983).
[8] Ando S, Sawada T, Inoue Y, *Electron. Lett.* 1993; **29**: 2143.
[9] Sawada T, Ando S, Sasaki S, *Appl. Phys. Lett.* 1999; **74**: 938.
[10] Matsuda S, Ando S, Sawada T, *Electron. Lett.* 2001; **37**: 706.
[11] Ando S, Sawada T, Sasaki S, *Polym. Adv. Tech.* 1999; **10**: 169.
[12] Ando S, Sawada T, Sasaki S, *Polym. Adv. Tech.* 2001; **12**: 319.
[13] Matsuura T, Hasuda Y, Nishi S, Yamada N, *Macromolecules* 1991; **24**: 5001.
[14] Boggess RK, Taylor LT, *J. Polym. Sci., Part A. Polym. Chem.* 1987; **25**: 685.
[15] Matsuda S, Ando S, (*submitted for publication*).
[16] Ricard D, Roussignol P, Flytzanis C, *Opt. Lett.* 1985; **10**: 511.
[17] Ogawa S, Hayashi Y, Kobayashi N, Tokizaki T, Nakamura A, *Jpn. J. Appl. Phys., Part 2* 1994; **33**: L331.